J. Biochem. 2010;148(1):35–46 doi:10.1093/jb/mvq031

JB THE JOURNAL OF BIOCHEMISTRY

Characterization of rice nucleotide sugar transporters capable of transporting UDP-galactose and UDP-glucose

Received December 13, 2009; accepted March 13, 2010; published online March 19, 2010

Junichi Seino[1,*], Kumiko Ishii[2], Takeshi Nakano[3,4], Nobuhiro Ishida[5], Masafumi Tsujimoto[6], Yasuhiro Hashimoto[1,†] and Shou Takashima[1,§]

[1]Glyco-chain Functions Laboratory, RIKEN-FRS, 2-1 Hirosawa, Wako, Saitama 351-0198, [2]Glycometabolome Team, RIKEN, 2-1 Hirosawa, Wako, Saitama 351-0198, [3]Plant Chemical Biology Research Unit, RIKEN, 2-1 Hirosawa, Wako, Saitama 351-0198 [4]Precursory Research for Embryonic Science and Technology (PRESTO), Japan Science and Technology Agency (JST), Chiyoda-ku, Tokyo 102-0075, [5]Department of Environmental Security System, Faculty of Risk and Crisis Management, Chiba Institute of Science, 3 Shiomi-cho, Choshi, Chiba 288-0025 and [6]Cellular Biochemistry Laboratory, RIKEN, 2-1 Hirosawa, Wako, Saitama 351-0198, Japan

*Junichi Seino, Glycometabolome Team, RIKEN, 2-1 Hirosawa, Wako, Saitama 351-0198, Japan.

†Yasuhiro Hashimoto, Department of Biochemistry, School of Medicine, Fukushima Medical University, 1 Hikarigaoka, Fukushima-shi, Fukushima 960-1295, Japan.

§Shou Takashima, Laboratory of Glycobiology, The Noguchi Institute, 1-8-1 Kaga, Itabashi, Tokyo 173-0003, Japan. Tel: +81-3-5944-3212, Fax: +81-3-3964-5588, email: staka@noguchi.or.jp

Using the basic local alignment search tool (BLAST) algorithm to search the *Oryza sativa* (Japanese rice) nucleotide sequence databases with the *Arabidopsis thaliana* UDP-galactose transporter sequences as queries, we found a number of sequences encoding putative *O. sativa* UDP-galactose transporters. From these, we cloned four putative UDP-galactose transporters, designated OsUGT1, 2, 3 and 4, which exhibited high sequence similarity with *Arabidopsis thaliana* UDP-galactose transporters. OsUGT1, 2, 3 and 4 consisted of 350, 337, 345 and 358 amino acids, respectively, and all of these proteins were predicted to have multiple transmembrane domains. To examine the UDP-galactose transporter activity of the OsUGTs, we introduced the OsUGTs' expression vectors into UDP-galactose transporter activity-deficient Lec8 cells. Our results showed that transfection with OsUGT1, 2 and 3 resulted in recovery of the deficit phenotype of Lec8 cells, but transfection with OsUGT4 did not. The results of an *in vitro* nucleotide sugar transport assay of OsUGTs, carried out with a yeast expression system, suggested that OsUGT4 is a UDP-glucose transporter rather than a UDP-galactose transporter. Although plants have multiple UDP-galactose transporter genes, phylogenic analysis indicates that plant UDP-galactose transporter genes are not necessarily evolutionary related to each other.

Keywords: Lec8 cell/nucleotide sugar transporter/*Oryza sativa*/UDP-galactose/UDP-glucose.

Abbreviations: BLAST, the basic local alignment search tool; CHO, Chinese hamster ovary; ER, endoplasmic reticulum; FITC, fluorescein isothiocyanate; Fuc, fucose; Gal, galactose; GalNAc, *N*-acetylgalactosamine; GAPDH, glyceraldehyde 3-phosphate dehydrogenase; Glc, glucose; GlcNAc, *N*-acetylglucosamine; MAM, *Maackia amurensis*; Man, mannose; NST, nucleotide sugar transporter; OsUGT, *Oryza sativa* UDP-galactose transporter; PBS, phosphate buffered saline; RT–PCR, reverse transcription polymerase chain reaction; Sia, sialic acid; TP, triose-phosphate.

Many glycosyltransferases are located in the membrane of the Golgi body and the endoplasmic reticulum (ER), with their catalytic sites facing the lumen of these organelles. Glycosyltransferases play a role in the synthesis of sugar chains, using nucleotide sugars as donor substrates. Although some nucleotide sugars, such as UDP-arabinose and UDP-galacturonic acid, are thought to be synthesized in the lumen of the Golgi body in plants (*1*, *2*), most nucleotide sugars are synthesized in the cytoplasm or, in the case of CMP-sialic acid (CMP-Sia) in animals, in the nucleus (*3*). Therefore, nucleotide sugars synthesized either outside the Golgi body or the ER have to be transported into the lumen of these organelles before they are utilized by glycosyltransferases as substrates for glycoconjugate biosynthesis; this transportation is brought about by nucleotide sugar transporters (NSTs). Like glycosyltransferases, NSTs are located in the membrane of the Golgi body and the ER, and carry nucleotide sugars into the lumen of these organelles as antiporters (*4*). They exchange the nucleotide sugar with the corresponding nucleotide monophosphate that is a product of the glycosylation reaction. In the case of animals, mainly humans, the NST family is designated as the solute carrier family 35 (SLC 35) (*5*). In plants, the chloroplast transporters for

triose-phosphate, phosphoenolpyruvate, glucose-6-phosphate and xylulose-5-phosphate show sequence similarity to NSTs, and both of them are classified into the same family, which is designated as the triose-phosphate/NST family (TP-NST) (*6*). At present, more than 40 members of the TP-NST gene family have been identified in the *Arabidopsis thaliana* genome (*7*, *8*), and some of them have been cloned and characterized (*8*–*13*).

UDP-galactose (UDP-Gal) transporters have been extensively analysed in *A. thaliana* NSTs (*8*, *10*–*12*). AtUTr1 was the first *A. thaliana* UDP-Gal transporter discovered, and by co-incidence it also happened to be a UDP-glucose (UDP-Glc) transporter (*10*). A database search predicted that at least five other genes in the *A. thaliana* genome encode for UDP-Gal transporters (AtUTr2–6) (*10*). One of them, AtUTr2, has also been proven to have UDP-Gal transporter activity (*11*). Other *A. thaliana* UDP-Gal transporters, AtUDP-GalT1 (*8*), AtUDP-GalT2 (*8*) and AtNST-KT1 (*12*) have also been reported. Although many *A. thaliana* UDP-Gal transporters have been characterized, little is known about UDP-Gal transporters from other plants. To improve this situation and to enable us to compare properties of UDP-Gal transporters from various plants, we analysed four putative UDP-Gal transporters from *Oryza sativa* (Japanese rice). Here, we report the cloning and characterization of *O. sativa* UDP-Gal transporters (OsUGTs) and discuss the evolutionary divergence of plant UDP-Gal transporters.

Experimental procedures

Materials

The [^{14}C]-labelled radioactive nucleotide sugars were purchased from Perkin Elmer; the exceptions were UDP-[^{14}C]*N*-acetylgalactosamine (UDP-[^{14}C]GalNAc) and CMP-[^{14}C]Sia, which were purchased from NEN Life Science Products and GE Healthcare, respectively. *Oryza sativa*. L. *japonica* cv. Nipponbare was cultivated for 3 weeks in potting soil irrigated with H_2O in a naturally lit greenhouse, and then harvested for RNA extraction.

Isolation of OsUGT cDNAs

Oryza sativa sequences exhibiting similarity with *A. thaliana* UDP-Gal transporters were identified through basic local alignment search tool (BLAST) algorithm searches against the translated nucleotide sequence databases (tBLASTn) at the National Centre for Biotechnology Information. Total RNA was extracted from 3-week-old *O. sativa* seedlings (total plant; leaves, leaf sheathes and roots) by using ISOGEN (Wako, Japan), and first-strand cDNA was synthesized using SuperScript II reverse transcriptase (Invitrogen). To obtain the entire coding regions of the two clones exhibiting the high similarity to AtUDP-GalT1 (At1g77610) (*8*), which we tentatively designated OsUGT1 (Os04g0692000) and OsUGT2 (Os08g0104900), reverse transcription–polymerase chain reaction (RT–PCR) was performed as follows. For the amplification of OsUGT1 cDNA, the following primers were used: 5′-GAGATG GAGCAGGGGGGTGAGGCCGGCACC-3′ (GF253+, nucleotides 310–399 in GenBank^{TM} accession No. AK061991) and 5′-TT GTTAAACCTTTTCTTGCTTGTCGCCTAC-3′ (GF254−, complementary to nucleotides 1,339–1,368 in GenBank^{TM} accession No. AK061991). For the amplification of OsUGT2 cDNA, the following primers were used: 5′-TGATCTCGATCTCGATCGATGG AGGAAGCC-3′ (GF259+, nucleotides 372–401 in GenBank^{TM} accession No. XM_507083) and 5′-TTTTAATTTGGTGGCCAATTA AATCTTCTC-3′ (GF260−, complementary to nucleotides 1,392–1,421 in GenBank^{TM} accession No. XM_507083). RT–PCR was performed as follows using *Pyrobest* DNA polymerase (Takara, Japan) with the first-strand cDNA of 3-week-old *O. sativa* seedlings (total plant) as a template: 94°C for 60 s; 35 cycles of 94°C for 30 s, 50°C for 60 s and 72°C for 90 s; and 72°C for 7 min. To obtain the entire coding regions of other clones exhibiting the highest similarity to AtUDP-GalT2 (At1g76670) (*8*) and AtUTr1 (At2g02810) (*10*), we tentatively designated OsUGT3 (Os07g0581000) and OsUGT4 (Os06g0593100), respectively, RT–PCR was performed as described above using primer sets, 5′- GGCGAGATGGAGGCGGAGAAGA AGCCGCCG-3′ (GF257+, nucleotides 141–170 in GenBank^{TM} accession No. XM_506427) and 5′- TAGCTAGCTCTTCATCTCGC CTTCCTCGAG-3′ (GF258−, complementary to nucleotides 1,158–1,187 in GenBank^{TM} accession No. XM_506427) for the amplification of OsUGT3 cDNA, and 5′-CGCCATGGTCACCGC GCGCAAGGGCCGCGG-3′ (GF245+, nucleotides 51–80 in GenBank^{TM} accession No. AK071175) and 5′-CTCATTCCTTGT GGTCTCTGACCTTCTTTC-3′ (GF246−, complementary to nucleotides 1,103–1,132 in GenBank^{TM} accession No. AK071175) for the amplification of OsUGT4 cDNA. Each PCR product was cloned into the *Eco*RV site of the pBluescript II SK(+) vector. The nucleotide sequences were confirmed by the dideoxy termination method by using an ABI 3100 DNA sequencer (Applied Biosystems).

Expression analysis of OsUGT genes

For expression analysis of the OsUGT genes, *O. sativa* seeds were placed in plastic tubes containing liquid Murashige and Skoog (MS) medium (*14*). These tubes were divided into two groups for germination. One group was placed at room temperature in a 16 h light/8 h dark cycle (light condition), and the other group was placed in an incubator at 28°C in the dark (dark condition). After 1 week of growth, the dark condition plantlets and part of the light condition plantlets were harvested for RNA extraction. The remaining light condition plantlets were transferred to potting soil irrigated with H_2O, and continued to grow under the light condition. These remaining plantlets were harvested for RNA extraction after 1, 2 and 3 weeks of growth. The plantlets were dissected into cotyledons, roots, leaves and leaf sheathes. Total RNA was extracted with an RNeasy Plant Mini Kit (QIAGEN), and first-strand cDNAs were synthesized with SuperScript III reverse transcriptase (Invitrogen). The relative expression levels of OsUGT mRNAs were estimated by RT–PCR. We used the first-strand cDNAs as templates and specific primers as described as above. Expression of the *O. sativa* glyceraldehyde-3-phosphate dehydrogenase (GAPDH) gene, which was used as the control, was also measured using the *O. sativa* GAPDH-specific primers 5′-AAAGGAGGCTTCTCTTACAGTG GCCAGAAG-3′ (CB400+, nucleotides 871–900 in GenBank^{TM} accession No. AF357884) and 5′-TCAGCCCATGGTGTAGGAT GGAGATGGTAG-3′ (CB401−, complementary to nucleotides 1,495–1,524 in GenBank^{TM} accession No. AF357884) (*15*). PCR was performed as follows using ExTaq Hot Start Version DNA polymerase (Takara, Japan): 98°C for 10 s; 35 cycles of 98°C for 10 s, 60°C (OsUGT1-3) or 50°C (OsUGT4) for 30 s, 72°C for 120 s (30 cycles were performed for GAPDH); and 72°C for 7 min. The PCR products were electrophoresed on a 2% agarose gel, stained with ethidium bromide and then visualized under UV light.

Construction of epitope-tagged expression vectors

The DNA fragment containing *Bgl*II and *Xba*I sites and the HA-epitope (YPYDVPDYA) tag-encoding sequence with the stop codon was synthesized by annealing the following primers, 5′-CTAG TAGATCTTCTAGATACCCCTACGATGTGCCCGATTACGC CTAAGC-3′ (GF283+) and 5′-GGCCGCTTAGGCGTAATCGG GCACATCGTAGGGGTATCTAGAAGATCTA-3′ (GF284−). The fragment was cloned into the *Spe*I–*Not*I sites of the pBluescript II SK(+) vector, yielding pBSSK-HA. The DNA fragment encoding the entire coding region of OsUGT1, but without the stop codon, was prepared by PCR amplification using the primers 5′-GAATTCATGGAGCAGGGGGGTGAGGCCGGC-3′ (GF295+, the synthetic *Eco*RI site is underlined) and 5′-TCTAGA AACCTTTTCTTGCTTGTCGCCTAC-3′ (GF296−, the synthetic *Xba*I site is underlined) with the cloned OsUGT1 cDNA fragment as a template, using the PCR conditions described above (see Isolation of OsUGT cDNAs section). The amplified fragment was digested with *Eco*RI and *Xba*I, and it was cloned into the *Eco*RI–*Xba*I sites of the pBSSK-HA vector. From this plasmid, the *Bgl*II–*Not*I fragment, which contains the HA-tagged entire coding region of OsUGT1, was prepared. This fragment was

subcloned into the *Eco*RI–*Not*I sites of the mammalian expression vector pcDNA 3.1/Myc-His A (Invitrogen), yielding pcDNA-OsUGT1. For the construction of the yeast expression vector, the above fragment was subcloned into the *Eco*RI–*Not*I sites of the yeast expression vector pYEX-BESN (*16*), yielding pYEX-OsUGT1.

The DNA fragment encoding the entire coding region of OsUGT2 but without the stop codon was prepared by PCR amplification using primers 5′-GGATCCCGATCTCGATCGATGGAGGAAG CC-3′ (GF297+, the synthetic *Bam*HI site is underlined) and 5′-TCTAGAAATCTTCTCTTGCTTGTCTCCTAC-3′ (GF298−, the synthetic *Xba*I site is underlined) with the cloned OsUGT2 cDNA fragment as a template and using the PCR conditions described above (see Isolation of OsUGT cDNAs section). The amplified fragment was digested with *Bam*HI and *Xba*I, and it was cloned into the *Bam*HI–*Xba*I sites of pBSSK-HA. From this plasmid, the *Bam*HI–*Not*I fragment, which contains the HA-tagged entire coding region of OsUGT2, was prepared. This fragment was subcloned into the *Bam*HI–*Not*I sites of pcDNA 3.1/Myc-His A, yielding pcDNA-OsUGT2. For the construction of the yeast expression vector, the above fragment was subcloned into the *Bam*HI–*Not*I sites of pYEX-BESN, yielding pYEX-OsUGT2.

The DNA fragment encoding the entire coding region of OsUGT3 but without the stop codon was prepared by PCR amplification using primers 5′-GAATTCATGGAGGCGGAGAAGAAGCCGC CG-3′ (GF299+, the synthetic *Eco*RI site is underlined) and 5′-TCTAGAGCTCTTCATCTCGCCTTCCTCGAG-3′ (GF300−, the synthetic *Xba*I site is underlined) with the cloned OsUGT3 cDNA fragment as a template and using the PCR conditions described above (see Isolation of OsUGT cDNAs section). The amplified fragment was digested with *Eco*RI and *Xba*I, and it was cloned into the *Eco*RI–*Xba*I sites of pBSSK-HA. From this plasmid, the *Eco*RI–*Not*I fragment, which contains the HA-tagged entire coding region of OsUGT3, was prepared. This fragment was subcloned into the *Eco*RI–*Not*I sites of pcDNA 3.1/Myc-His A, yielding pcDNA-OsUGT3. For the construction of the yeast expression vector, the above fragment was subcloned into the *Eco*RI–*Not*I sites of pYEX-BESN, yielding pYEX-OsUGT3.

The DNA fragment encoding the entire coding region of OsUGT4 but without the stop codon was prepared by PCR amplification using primers 5′-GAATTCATGGTCACCGCGCGCAAGGGCC GC-3′ (GF303+, the synthetic *Eco*RI site is underlined) and 5′-TCTAGATTCCTTGTGGTCTCTGACCTTCTT-3′ (GF304−, the synthetic *Xba*I site is underlined) with the cloned OsUGT4 cDNA fragment as a template and using the PCR conditions described above (see Isolation of OsUGT cDNAs section). The amplified fragment was digested with *Eco*RI and *Xba*I, and it was cloned into the *Eco*RI–*Xba*I sites of pBSSK-HA. From this plasmid, the *Eco*RI–*Not*I fragment, which contains the HA-tagged entire coding region of OsUGT4, was prepared. This fragment was subcloned into the *Eco*RI–*Not*I sites of pcDNA 3.1/Myc-His A, yielding pcDNA-OsUGT4. For the construction of the yeast expression vector, the above fragment was subcloned into the *Eco*RI–*Not*I sites of pYEX-BESN, yielding pYEX-OsUGT4.

For the construction of the expression vector of human UDP-Gal transporter, the DNA fragment encoding the entire coding region of hUGT1 (*17*) but without the stop codon was prepared by PCR amplification using primers 5′-GAATTCATGGCAGCGGTTGGGGC TGGTGGT-3′ (GF305+, the synthetic *Eco*RI site is underlined) and 5′-TCTAGAGGAACCCTTCACCTTGGTGAGCAA-3′ (GF306−, the synthetic *Xba*I site is underlined) with the cloned hUGT1 cDNA fragment as a template and using the PCR conditions described above (see Isolation of OsUGT cDNAs section). The amplified fragment was digested with *Eco*RI and *Xba*I, and it was cloned into the *Eco*RI–*Xba*I sites of pBSSK-HA. From this plasmid, the *Eco*RI–*Not*I fragment, which contains the HA-tagged entire coding region of hUGT1, was prepared. This fragment was subcloned into the *Eco*RI–*Not*I sites of pcDNA 3.1/Myc-His A, yielding pcDNA-hUGT1. For the construction of the yeast expression vector, the above fragment was subcloned into the *Eco*RI–*Not*I sites of pYEX-BESN, yielding pYEX-hUGT1.

Assessment of UDP-Gal transporter activity using Lec8 cells

The Chinese hamster ovary (CHO) cell line UDP-Gal transporter activity-deficient mutant, Lec8 (*18*), was cultured in minimum essential medium α supplemented with 10% fetal calf serum. Lec8 cells were transiently transfected with the abovementioned pcDNA vectors by using the FuGENE 6 reagent (Roche Diagnostics) and cultured for 2 days in a chamber slide. Cells were fixed with 3% paraformaldehyde for 20 min and washed twice with phosphate buffered saline (PBS). The fixed cells were incubated with 20 μg/ml of fluorescein isothiocyanate (FITC)-conjugated *Maackia amurensis* (MAM) lectin (EY Laboratories) for 1 h and washed four times with PBS. Fluorescence labelling was visualized under an IX71 fluorescent microscope (OLYMPUS).

Yeast strain, transformation and culture

Saccharomyces cerevisiae strain YPH500 (*MATα, ura3-52, lys2-801, ade2-101, trp1-Δ63, his3-Δ200, leu2-Δ1*) was used in the expression study. Yeast transformation was performed using the lithium acetate method as previously described (*19*), and the yeast expression vectors were constructed as described above. Transformants were selected with a selective medium containing 0.67% Bacto-yeast nitrogen base without amino acids, 2% glucose (YNBD) and auxotrophic supplements, except uracil. For preparation of the membrane vesicles, the transformants were grown in liquid selective medium until they reached a density of $A_{600} = 0.4$. Cupric sulphate was then added to the culture media at a final concentration of 0.5 mM to induce expression of the introduced OsUGT gene, which was under the control of the copper ion-inducible *CUP1* promoter. The cells were further cultured for 2 h and then harvested.

Preparation of yeast membrane vesicles

Preparation of membrane vesicles was carried out as previously described (*20*). Cells were washed with ice-cold 10 mM NaN_3 and converted into spheroplasts with a spheroplast preparation solution containing 1.4 M sorbitol, 50 mM potassium phosphate (pH 7.5), 10 mM NaN_3, 0.25% (v/v) 2-mercaptoethanol and 2 mg of Zymolyase-100T (SEIKAGAKU Corp., Japan) per gram of cells by incubation at 37°C for 20 min. The spheroplasts were collected as a pellet and resuspended in five volumes of lysis buffer containing 0.8 M sorbitol, 10 mM HEPES–Tris (pH 7.4), 1 mM EDTA and a protease-inhibitor cocktail (Complete, EDTA-free; Roche Diagnostics). The spheroplasts were homogenized by passing them several times through a 200-μl micropipette tip attached to a serological pipette. The lysate was centrifuged at 1,500*g* for 10 min to remove the intact cells and debris. The supernatant was centrifuged at 100,000*g* for 60 min to yield a pellet of membrane vesicles, P100 (precisely, P10 + P100). The P100 fractions were resuspended in the lysis buffer.

Western blot analysis

Western blotting was carried out as previously described (*21*). The HA-tagged proteins were detected with the rat anti-HA monoclonal antibody 3F10 (Roche Diagnostics).

Assessment of NST activity by using yeast membrane vesicles

The transport assay using yeast membrane vesicles was performed essentially as previously described (*22*, *23*). Briefly, 100 μl of the transport reaction mixture contained yeast membrane vesicles equivalent to 50 μg total protein, 5–10 μM [^{14}C]-radiolabelled substrate, 0.8 M sorbitol, 10 mM Tris–HCl (pH 7.0) and 0.5 mM dimercaptopropanol. The reaction mixture was incubated at 30°C. The reaction was initiated by the addition of membrane vesicles and terminated after 1 min by an 11-fold dilution with an ice-cold stop buffer containing 0.8 M sorbitol, 10 mM Tris–HCl (pH 7.0) and 1 μM non-radiolabelled substrate. The entire reaction mixture was filtered through a nitrocellulose filter, washed three times with 1 ml of the ice-cold stop buffer, and dried. The radioactivity trapped on the filter was measured with a toluene-based scintillator.

Indirect immunofluorescence studies

For immunofluorescence analysis, we seeded Lec8 cells onto glass cover slips. Cells were transiently transfected with the above mentioned pcDNA-OsUGT expression vectors by using AMAXA Nucleofector II according to the manufacturer's instructions. After cultivation for 2 days, cells were fixed with 3% paraformaldehyde for 20 min and washed three times with PBS. Then samples were incubated with 50 mM NH_4Cl for 10 min for quenching, and washed three times with PBS. Permeabilization was carried out with 0.1% Triton X-100 for 10 min, and washed 3 times with PBS. After permeabilization, samples were blocked with PBS containing

0.5% bovine serum albumin for 30 min, followed by incubation with the respective primary antibodies for 1 h [mouse anti-HA monoclonal antibody (1:100; F-7, Santa Cruz) and rabbit anti-calnexin polyclonal antibody (1:500; Stressgen) or rabbit anti-HA polyclonal antibody (1:100; Y-11, Santa Cruz) and mouse anti-GM130 monoclonal antibody (1:200; BD Bioscience)]. Samples were washed three times with PBS and incubated with the respective following fluorochrome conjugated secondary antibodies (1:500) for 30 min (goat anti-mouse IgG conjugated to Alexa Fluor 488 and goat anti-rabbit IgG conjugated to Alexa Fluor 555 or goat anti-rabbit IgG conjugated to Alexa Fluor 488 and goat anti-mouse IgG conjugated to Alexa Fluor 555; Invitrogen). Then samples were washed three times with PBS and once with water, and dried. The dried cover slips were mounted in Mowiol (Calbiochem) and analysed under an OLYMPUS FV1000 conforcal microscope.

Results and discussion

Cloning cDNA of OsUGT1, 2, 3 and 4

We used the BLAST algorithm to search the *O. sativa* nucleotide sequence databases with the *A. thaliana* UDP-Gal transporter sequences [AtUDP-GalT1 (*8*), AtUDP-GalT2 (*8*), and AtUTr1 (*10*)] as queries. We found a number of sequences encoding putative *O. sativa* UDP-Gal transporters. From these, we cloned two cDNA clones that exhibited high similarity with the AtUDP-GalT1; the cloning was conducted by RT–PCR. One cDNA encoded a 322-amino acid protein with a calculated molecular mass of 38,462 Da, which we designated as OsUGT1. OsUGT1 shared 81.6% of its amino acid sequence with AtUDP-GalT1 (Table I). The other cDNA encoded a 337-amino acid protein with a calculated molecular mass of 37,809 Da, which we designated as OsUGT2. OsUGT2 shared 82.5% of its amino acid sequence identity with AtUDP-GalT1 (Table I). In addition to these clones, we also obtained two cDNA clones, whose deduced amino acid sequences exhibited high similarity with AtUDP-GalT2 and AtUTr1, respectively. One cDNA encoded a 345-amino acid protein with a calculated molecular mass of 37,385 Da, which we designated as OsUGT3. OsUGT3 shared 70.1% of its amino acid sequence with AtUDP-GalT2 (Table I). The other cDNA encoded a 358-amino acid protein with a calculated molecular mass of 39,520 Da, which we designated as OsUGT4. OsUGT4 shared 72.8% of its amino acid sequence with AtUTr1 (Table I). Of the four OsUGT clones, none showed any sequence similarity with each other except OsUGT1 and OsUGT2 (Table I).

It has been demonstrated that mouse CMP-Sia transporter has 10 transmembrane domains with both the N- and C-termini facing the cytoplasm (*24*). Hydropathy analysis of other NSTs predicted that they also share this topology. For example, human UDP-Gal transporter (hUGT1) has been predicted to have 10 transmembrane domains (*25*, *26*). We predicted the topology of OsUGT1, 2, 3 and 4 by using TOPCONS algorithm (http://topcons.cbr.su.se/) (*27*) (Fig. 1). The prediction made by TOPCONS is a consensus from five different topology prediction algorithms: SCAMPI (single sequence mode) (*28*), SCAMPI (multiple sequence mode) (*28*), PRODIV-TMHMM (*29*), PRO-TMHMM (*29*) and OCTOPUS (*30*). These five predictions are used as input to the TOPCONS hidden Markov model, which gives a consensus prediction for the protein, together with a reliability score based on the agreement of the included methods across the sequence. The consensus topology model is shown schematically in the upper part of each column (Fig. 1). In addition, ZPRED (*31*) is used to predict the *Z*-coordinate (*i.e.* the distance to the membrane centre) of each amino acid, and ΔG-scale (*32*) is used to predict the free energy of membrane insertion for a window of 21 amino acids centred around each position in the sequence. TOPCONS algorithm predicted that OsUGT1, 2, and 3 had 10 transmembrane domains like hUGT1 (Fig. 1). The transmembrane helices were predicted to locate where both the *Z*-coordinate and the free energy values were low. The behaviour of the *Z*-coordinate curve coincided well with that of the free energy curve for OsUGT1, 2 and 3. However, the behaviour of the *Z*-coordinate curve did not coincide with that of the free energy curve in some parts for OsUGT4. As a result, OsUGT4 was predicted to have eight transmembrane domains (Fig. 1). AtUTr1, a homolog of OsUGT4, was also predicted to have eight transmembrane domains (*10*).

The *OsUGT1* gene is located on *O. sativa* chromosome 4, spans over 2 kb of genomic DNA and consists of five exons. The *OsUGT2* gene is located on *O. sativa* chromosome 8, spans over 2.6 kb of genomic DNA, and consists of five exons. The genomic structures of these two genes are very similar (Fig. 2). The amino acid sequence similarity and the genomic structural resemblance of the *OsUGT1* and *OsUGT2* genes suggest that they have arisen from a common ancestral gene. Like the *OsUGT1* and *OsUGT2* genes, the *OsUGT3* gene, which is located on *O. sativa* chromosome 7, spans over 3 kb of genomic DNA, and consists of

Table I. Comparison of amino acid sequences of OsUGT1–4 proteins and *A. thaliana* UDP-Gal transporters.

	OsUGT1	OsUGT2	OsUGT3	OsUGT4	AtUDP-GalT1	AtUDP-GalT2	AtUTr1	AtNST-KT1
OsUGT1	100	84.4	ns	ns	81.6	ns	ns	ns
OsUGT2		100	ns	ns	82.5	ns	ns	ns
OsUGT3	–	–	100	ns	ns	70.1	ns	50.2
OsUGT4	–	–	–	100	ns	ns	72.8	ns
AtUDP-GalT1	–	–	–	–	100	ns	ns	ns
AtUDP-GalT2	–	–	–	–	–	100	ns	50.3
AtUTr1	–	–	–	–	–	–	100	ns
AtNST-KT1	–	–	–	–	–	–	–	100

The amino acid sequence identity (%) is shown.
ns: no significant similarity

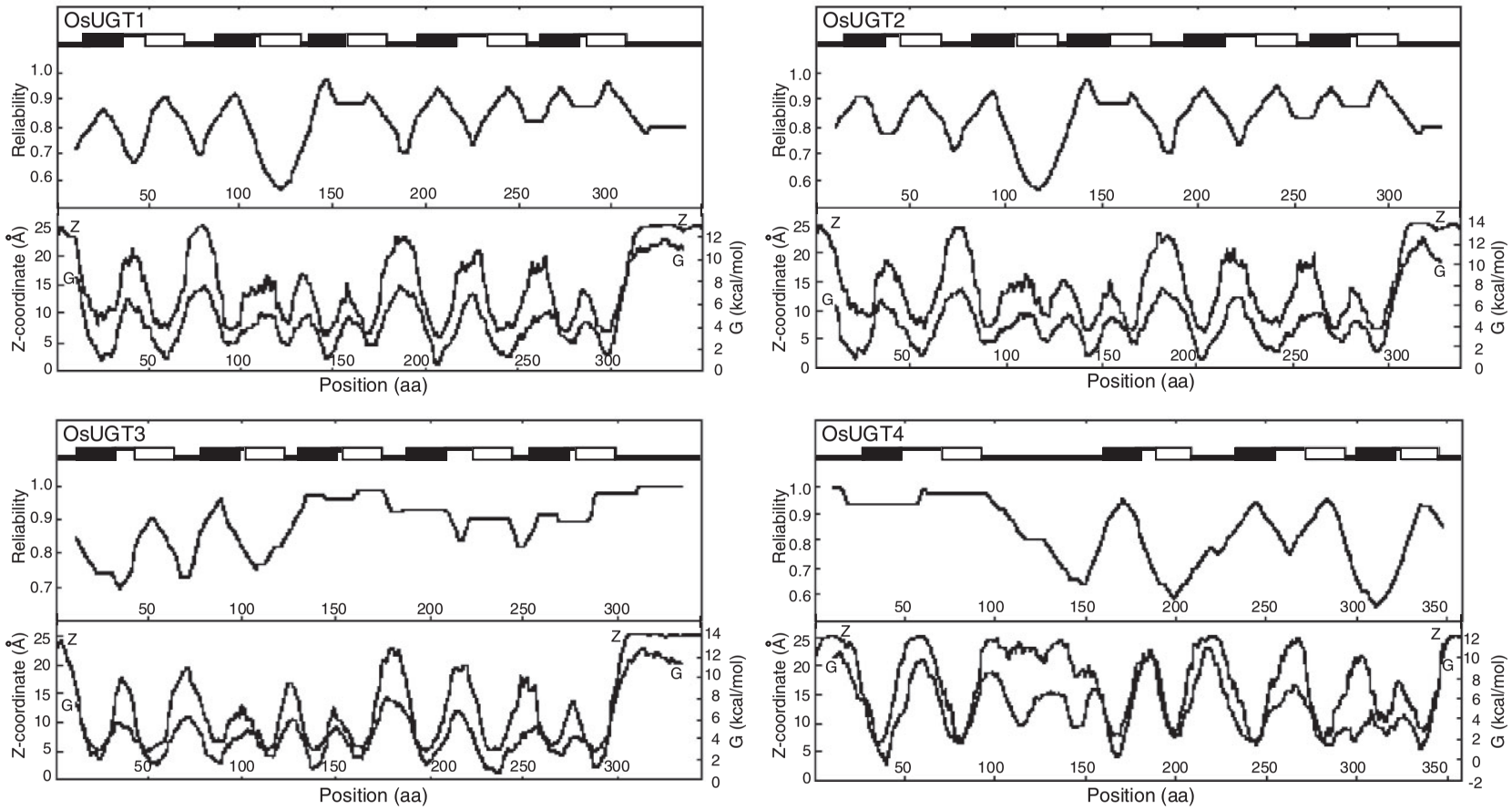

Fig. 1 Topology prediction of OsUGT1–4. The topology models are based on TOPCONS prediction algorism (*27*). In the upper part of each column, the consensus topology model is shown schematically, together with its reliability score. Transmembrane domains are shown by filled (in to out direction) and open (out to in direction) rectangles. The *Z*-coordinate (*Z*, the distance to the membrane centre) and the free energy for membrane insertion (G) were also predicted.

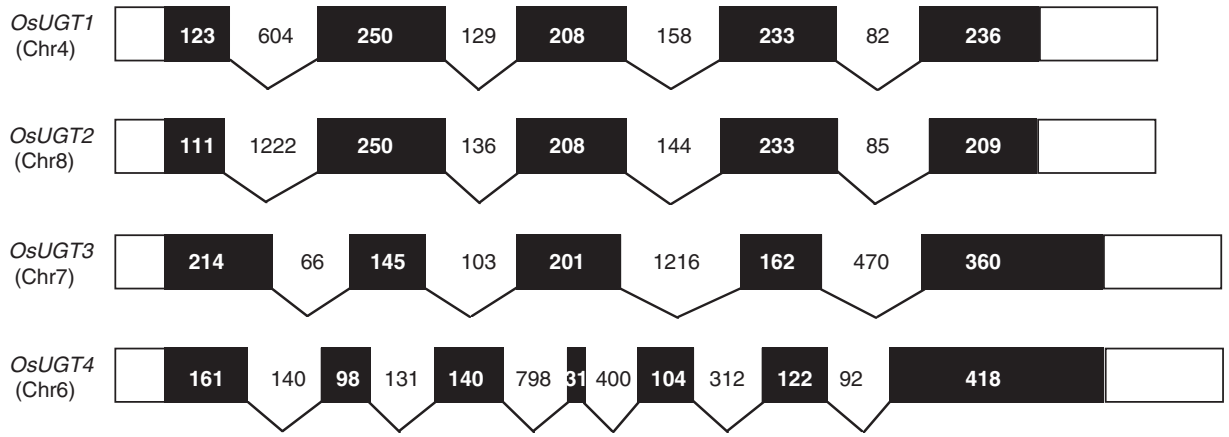

Fig. 2 Comparison of the genomic structures of *OsUGT1–4* genes. The genomic structures of *OsUGT1–4* genes are presented. Exons are represented by rectangles, and coding regions are shaded. Untranslated regions are not necessarily shown to scale. Numbers indicate the size of each region in base pairs.

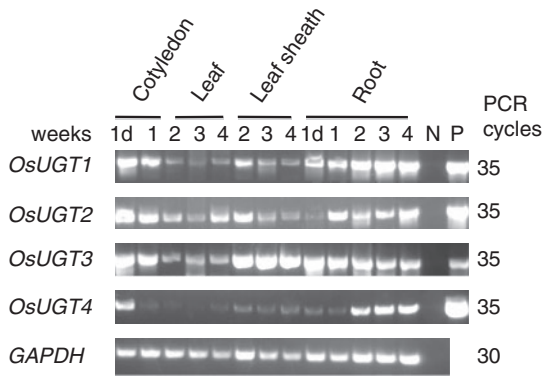

Fig. 3 Expression analysis of *OsUGT1–4* genes. Relative expression levels of *OsUGT1–4* genes during the development of *O. sativa* seedlings were measured by RT–PCR. 1d: plantlets were grown under the dark condition for 1 week. N: negative control, in which RT–PCR was performed without the template cDNA. P: positive control, in which RT–PCR was performed using the cloned cDNA of corresponding *OsUGT* gene as a template.

five exons. However, each exon size in the *OsUGT3* gene is different than the size of the corresponding exons in the *OsUGT1* and *OsUGT2* genes. Since the amino acid sequence of OsUGT3 dissimilar to those of OsUGT1 and OsUGT2, it seems that the *OsUGT3* gene evolved separately from the *OsUGT1* and *OsUGT2* genes. Similarly, the *OsUGT4* gene, which is located on *O. sativa* chromosome 6, spans over 3 kb of genomic DNA, and consists of seven exons, also seems to have evolved separately from the *OsUGT1*, *OsUGT2* and *OsUGT3* genes.

The developing *O. sativa* seedlings expressed these genes ubiquitously, but the expression level of each gene differed from tissue to tissue, and varied depending on the plants' cultivation condition (Fig. 3). For example, the expression of the *OsUGT1* gene in root and cotyledon tissues was relatively high compared to its expression in other tissues. The expression of the *OsUGT3* gene in leaf tissues was relatively low compared to its expression in other tissues. In the case of the *OsUGT2* gene, its expression in root tissue was suppressed under the dark condition. The expression of the *OsUGT4* gene was also ubiquitous, but its expression in leaf tissues was very low. In addition to examining the tissues, we searched the expressed sequence tag (EST) database and found that these genes were also expressed in tissues such as flower (panicle) and callus.

OsUGT1, 2 and 3 are able to complement Lec8 cells deficient in Golgi UDP-Gal transport

Since OsUGT1, 2, 3 and 4 demonstrated significant sequence similarity with *A. thaliana* UDP-Gal transporters, we examined the UDP-Gal transporter activity of these proteins with Lec8 cells, which are UDP-Gal transporter activity-deficient mutants of CHO cells (*18*). In Lec8 cells, UDP-Gal is not incorporated into the lumen of the Golgi body because these cells lack UDP-Gal transporter activity on the Golgi body membrane. Therefore, the endogenous Golgi body-resident galactosyltransferases cannot utilize UDP-Gal as a donor substrate. As a result, Lec8 cells do not express sialylglycoconjugates on their cell surface because of the lack of available galactose residue acceptor substrates for endogenous sialyltransferases. FITC-conjugated MAM lectin normally cannot stain Lec8 cells because this lectin binds Siaα2,3Gal residues (Fig. 4). However, Lec8 cells producing the active form of human UDP-Gal transporter were able to complement their UDP-Gal transporter activity and expressed α2,3-sialylglycoconjugates on their cell surfaces (Fig. 4). Lec8 cells transiently transfected with the expression vector for OsUGT1, *i.e.* pcDNA-OsUGT1, successfully expressed the corresponding protein (Fig. 5), and MAM lectin staining showed that α2,3-sialylglycoconjugates were expressed on the surface of OsUGT1-expressing cells (Fig. 4). Similar results were obtained with OsUGT2 and OsUGT3. However, positive staining results were not observed in the cells transfected with OsUGT4, despite the recombinant protein production of OsUGT4 in Lec8 cells (Figs 4 and 5). These results show that introduction of OsUGT1, OsUGT2 and OsUGT3 can rescue the phenotype of the Lec8 cells, but introduction of OsUGT4 does not show this effect.

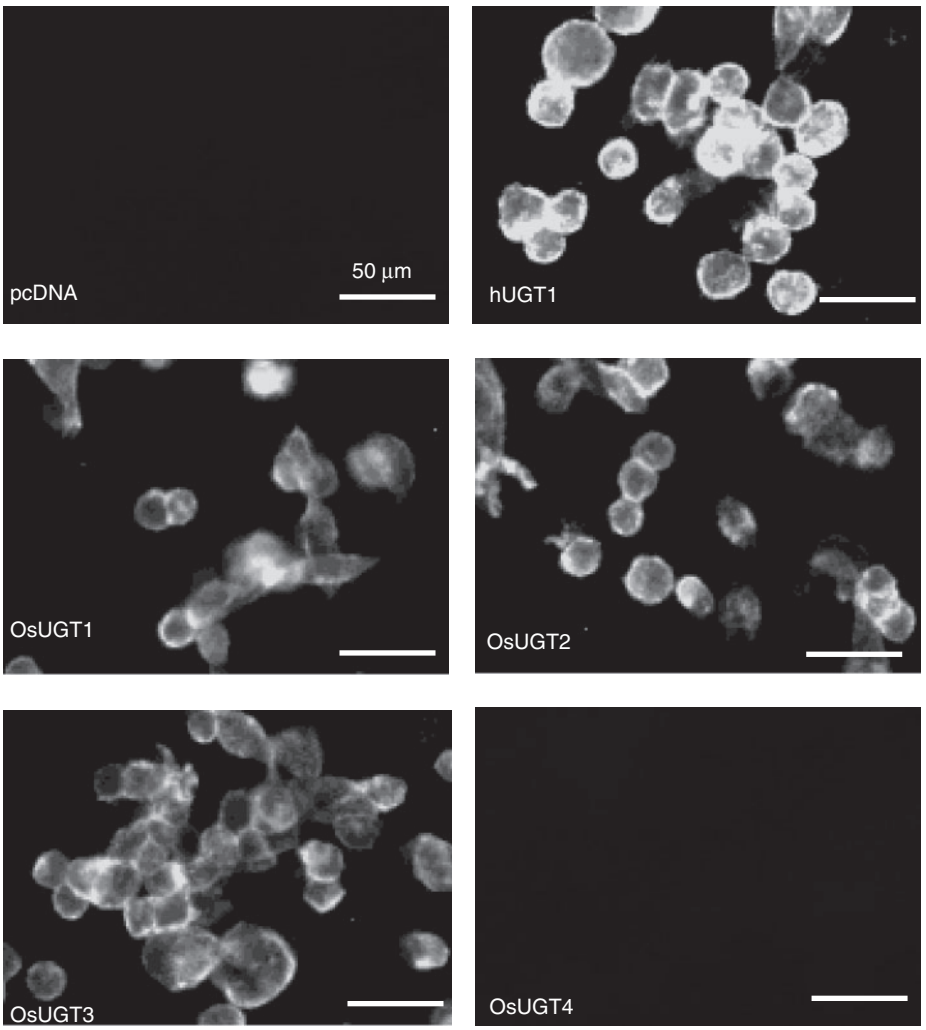

Fig. 4 Transient expression analysis to assess the UDP-Gal transporter activity of OsUGT1–4 proteins. Lec8 cells were transfected with the control empty vector (pcDNA) or expression vectors for human UDP-Gal transporter (hUGT1) or OsUGT1–4 proteins. Two days after transfection, the cells were stained with FITC-conjugated MAM lectin. Bar, 50 μm.

Production and measurement of NST activity of OsUGT1, 2, 3 and 4 with a yeast expression system

To further examine the NST activity of OsUGT1, 2, 3 and 4, we expressed these proteins in the yeast *Saccharomyces cerevisiae*. In general, yeast microsomal membranes have very low intrinsic NST activity, except for GDP-mannose (GDP-Man) transporting activity and UDP-Glc transporting activity, which are both potent in yeast. Therefore, yeast microsomal membrane fractions can be used for assaying most *in vitro* NST activity. We measured the incorporation of radiolabelled nucleotide sugars into yeast membrane vesicles in this assay.

The yeast expression vectors pYEX-OsUGT1, 2, 3 and 4, each of which contained the cDNA encoding the corresponding OsUGT tagged with an HA epitope at the C-terminus, were used for yeast transformation. We prepared the membrane fractions containing HA-tagged OsUGT1, 2, 3 and 4 from transformed cells grown in YNBD medium after induction with 0.5 mM $CuSO_4$ (Fig. 5) and used for the *in vitro* NST assay. For background control and a positive control, we used the membrane fractions prepared from cells transformed with an empty vector (pYEX-BESN) and an expression vector for human UDP-Gal transporter (pYEX-hUGT), respectively. The apparent molecular masses of the recombinant UGTs produced in both Lec8 and yeast cells were lower than the molecular masses predicted from the primary sequence of the protein plus the HA epitope tag (Fig. 5). However, a difference has been found between the predicted and apparent molecular masses of NSTs (*10*, *11*, *33*). Since NSTs have multiple transmembrane domains and are very hydrophobic, strong hydrophobic interactions that overcome the dissociation effect of SDS may occur, and NSTs may take a shrunken conformation that can migrate faster than the completely extended conformation of the SDS–protein on SDS–PAGE.

As shown in Fig. 6, we observed higher levels of UDP-Gal incorporated into the OsUGT-containing membrane vesicles than into the control membrane vesicles. In addition, we also observed higher levels of UDP-Glc incorporated into OsUGT1, OsUGT2 and OsUGT4-containing membrane vesicles than

into the control membrane vesicles. In this case, the OsUGT4-containing membrane vesicles exhibited the highest level of incorporation among the examined membrane vesicles. The incorporation of other nucleotide sugars into the OsUGT-containing membrane vesicles was nearly equal to, or lower than, their incorporation into the control membrane vesicles. It should be noted that the observed incorporation of radiolabelled nucleotide sugars into yeast membrane vesicles may have included some non-specific binding of radiolabelled nucleotide sugars to the introduced OsUGTs, which would have been indistinguishable from the NST uptake by OsUGTs, in this assay system. However, when taken together with the results of the experiment in the Lec8 cells, these results indicated that OsUGT1, 2 and 3 possess UDP-Gal transporter activity and incorporate UDP-Gal into the lumen of the Golgi body, and that some of OsUGTs might also transport other nucleotide sugars such as UDP-Glc. It should be noted that the *A. thaliana* UDP-Gal transporter AtUDP-GalT1, which is a homologue of OsUGT1 and OsUGT2, exhibits high UDP-Gal transporter activity but very low UDP-Glc transporter activity (*8*). Therefore, it could be said that wide substrate specificity is one of characteristics of OsUGT1 and 2.

On the other hand, it has been reported that AtUTr1, a homolog of OsUGT4, exhibits both UDP-Gal and UDP-Glc transporter activity (*10*). In our experiments, OsUGT4 also exhibited both UDP-Gal and UDP-Glc transporter activity *in vitro* (Fig. 6), but introduction of OsUGT4 in Lec8 cells did not rescue the phenotype of the Lec8 cells (Fig. 4). Although AtUTr1 displays both UDP-Gal and UDP-Glc transporter activity, its main function is as an ER-localized UDP-Glc transporter involved in quality control in the ER (*34*, *35*). An NST that localizes in the Golgi body and has UDP-Gal transporter activity is required to rescue the phenotype of

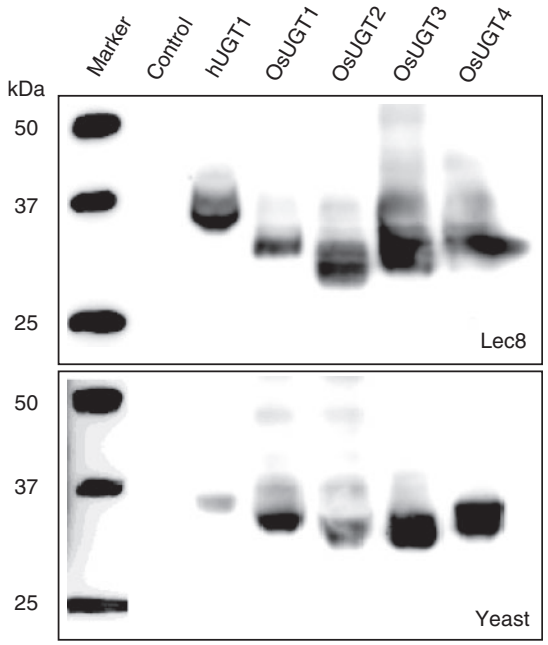

Fig. 5 Detection of recombinant NSTs in mammalian and yeast microsomal membranes. Microsomes were prepared from transfected Lec8 cells or transformed yeast cells. Samples, containing 10 μg of protein, were subjected to western blot analysis. Upper panel: proteins from Lec8 cells transfected with the empty pcDNA vector (control), hUGT1 expression vector, and OsUGT1–4 expression vectors. Lower panel: proteins from yeast cells transformed with the empty pYEX-BESN vector (control), hUGT1 expression vector and OsUGT1–4 expression vectors.

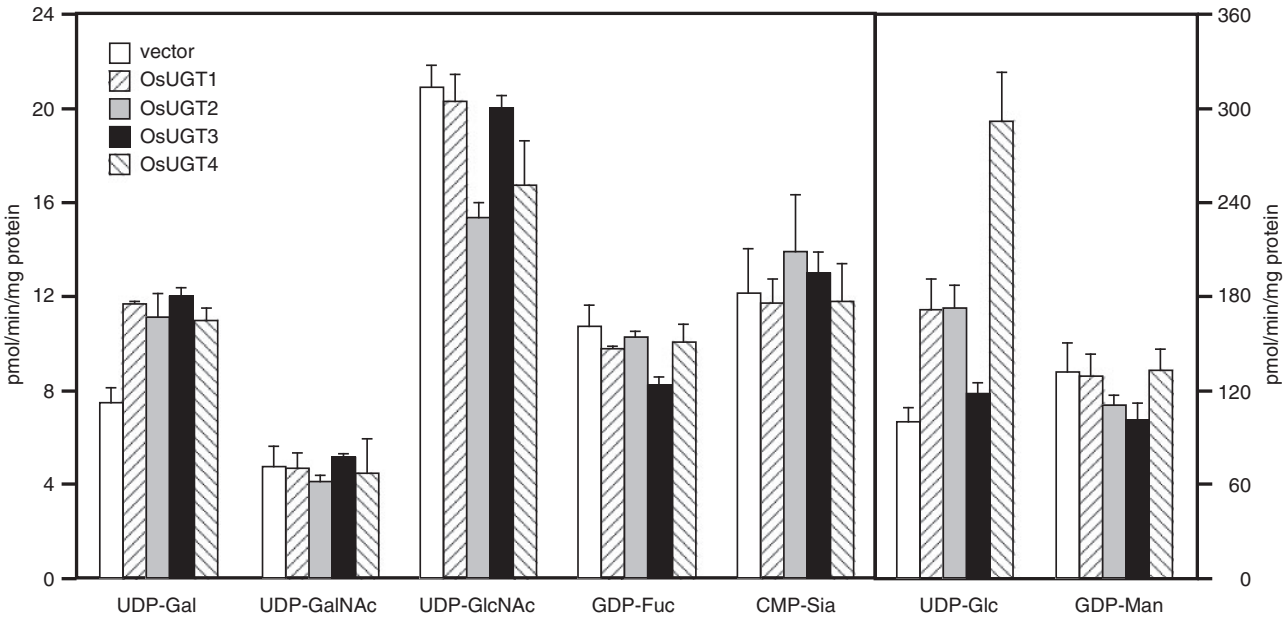

Fig. 6 NST activity of OsUGT1–4 proteins. Microsomes were prepared from yeast transformants and used for the NST assay with [^{14}C]-labelled UDP-Gal and various [^{14}C]-labelled nucleotide sugars as indicated below the columns. The uptake of substrate into microsomal vesicles was determined as described in Materials and Methods section and presented as incorporated nucleotide sugars (pmol)/min/mg protein used in assays. To determine the nucleotide sugar incorporation due to the activity of the introduced NST, the incorporation of introduced NST-containing microsomal vesicles was compared with that of vector-control microsomal vesicles.

the Lec8 cells. Therefore, if OsUGT4 localizes in the ER and has the same function as AtUTr1, this could explain OsUGT4's inability to rescue the phenotype of the Lec8 cells.

Intracellular localization of OsUGT1, 2, 3 and 4

We transiently expressed C-terminally HA-tagged constructs of OsUGT1, 2, 3 and 4 in Lec8 cells and analysed their intracellular localization by immunofluorescence. As shown in Fig. 7 (see also Supplementary Data), HA-tagged OsUGT1, 2 and 3 clearly colocalized with the Golgi marker GM130, whereas HA-tagged OsUGT4 mainly colocalized with the ER marker calnexin. It has been shown that the C-terminal dilysine motif (KKXX or KXKXX, where X denotes any amino acid) acts as an ER retention signal (*36*). For example, this motif is related to the ER retention of the large splice variant of the human UDP-Gal transporter (KVKGS) (*37*). The C-terminal sequence of AtUTr1 is YQIYLKWKKLQRVE KKKQKS, and that of OsUGT4 is GLSLQIFL KWKRKKVRDHKE. Although these sequences do not have typical dilysine motifs, their lysine-rich sequences may signal ER retention of these NSTs. Taken together with the high UDP-Glc transporter activity of OsUGT4 among examined OsUGTs (Fig. 6), and its high sequence similarity with AtUTr1 (72.8%), it is likely that OsUGT4 acts as an ER-resident UDP-Glc transporter *in vivo*, rather than a UDP-Gal transporter, and that is why OsUGT4 could not rescue the phenotype of Lec8 cells.

Phylogenic relation of plant UDP-Gal transporters

With sequences of *A. thaliana* and *O. sativa* UDP-Gal transporters, and animal NSTs having UDP-Gal transporter activity, we constructed a phylogenic unrooted tree of plant UDP-Gal transporter candidates with the ClustalW and the TreeView programs (*38*, *39*). As shown in Fig. 8, plant UDP-Gal transporters can be grouped into subfamilies. A multiple alignment search of plant UDP-Gal transporter sequences failed to show common motifs or conserved amino acid residues among plant UDP-Gal transporters. It is likely that these subfamilies are not evolutionarily related to each other. Nevertheless, these proteins all express UDP-Gal transporter activity, although some of them also transport other nucleotide sugars, such as UDP-Glc. Structural studies of these proteins will help elucidate common features necessary for expressing UDP-Gal transporter activity.

Why do plants need so many different species of UDP-Gal transporters? In plants, galactose is a component of both cell wall polysaccharides and of the carbohydrate moieties of glycoproteins and glycolipids. As galactose is essential carbohydrate for both plant structure and function, plants may generate several UDP-Gal transporter genes in order to avoid the damage that may be caused by the loss of function of a single UDP-Gal transporter gene. It is also possible that several UDP-Gal transporter genes are necessary for fine control of the expression of galactose-containing sugar chains. Fine control of sugar chain expression would allow for developmental stage- and tissue-specific glycosylation patterns. Yet at the present time, the biological significance of these multiple genes is unclear. Characterization of each UDP-Gal transporter, with knockout/knockdown experiments and analysis of the transcriptional regulation of each gene, will elucidate the biological significance of each UDP-Gal transporter and will clarify the reasons for diversity in plant UDP-Gal transporter genes.

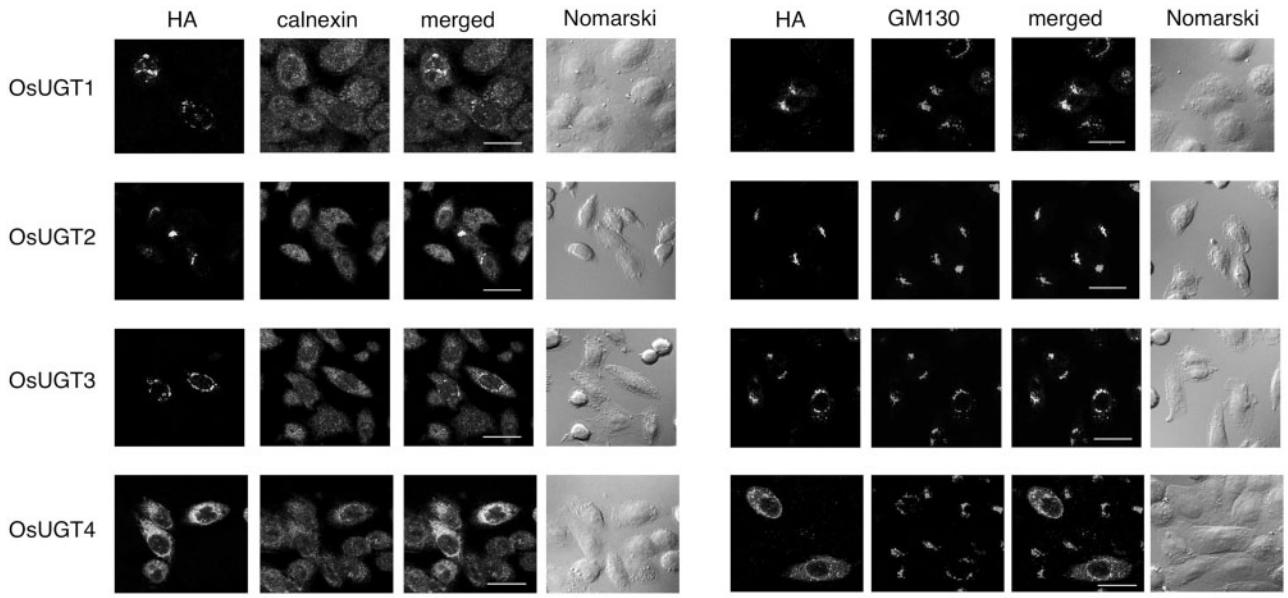

Fig. 7 Intracellular localization of OsUGT1–4. HA-tagged OsUGT1–4 proteins were transiently expressed in Lec8 cells, and the intracellular localization was compared with a Golgi (GM130) and an ER (calnexin) marker. Nomarski images of the same field were recorded in the transmission mode. Bar, 20 μm.

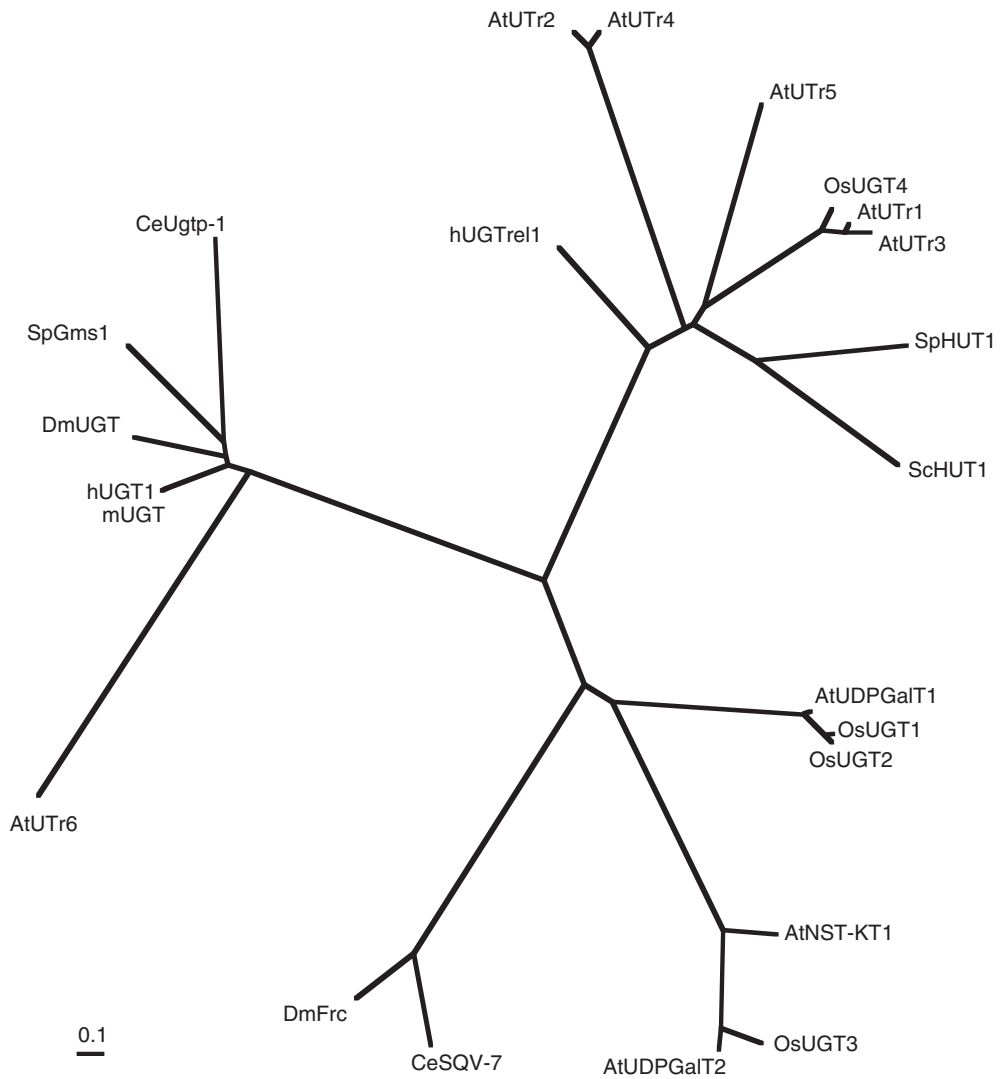

Fig. 8 Phylogenic relation of NSTs having UDP-Gal transporter activity. With sequences of putative plant UDP-Gal transporters and animal NSTs having UDP-Gal transporter activity, we constructed a phylogenic unrooted tree of plant UDP-Gal transporter candidates. The deduced amino acid sequence information was obtained from the following DDBJ/GenBank™/EBI Data Bank accession numbers: OsUGT1, AK061991; OsUGT2, XM_507083; OsUGT3, XM_506427; OsUGT4, AK071175; AtUTr1, NM_126336; AtUTr2, NM_118430; AtUTr3, NM_101303; AtUTr4, NM_101130; AtUTr5, NM_114487; AtUTr6, NM_115798; AtNST-KT1, NM_120099; AtUDPGalT1, NM_106409; AtUDPGalT2, NM_106317; hUGT1, NM_005660; hUGTrel1 (human UDP-Gal transporter-related protein 1), NM_005827; mUGT (mouse UDP-Gal transporter), NM_001083937; DmUGT (*Drosophila melanogaster* UDP-Gal transporter), NM_130663; DmFrc (*D. melanogaster* Fringe connection), NM_001144490; CeSQV-7 (*Caenorhabditis elegans* squashed vulva-7), NM_063035; CeUgtp-1 (*C. elegans* UDP-Gal transporter protein 1), NM_066529; ScHUT1 (*Saccharomyces cerevisiae* HUT1), AY692836; SpHUT1 (*Schizosaccharomyces pombe* HUT1), NM_001021157; SpGms1 (*S. pombe* Gms1), NM_001023033.

Supplementary Data

Supplementary Data are available at *JB* Online.

Funding

Sumitomo Foundation (to S.T., partial); Program for Promotion of Basic Research Activities for Innovation Bioscience (PROBRAIN) (to T.N.).

Conflict of interest

None declared.

References

1. Burget, E.G., Verma, R., Mølhøj, M., and Reiter, W.-D. (2003) The biosynthesis of L-arabinose in plants. Molecular cloning and characterization of a golgi-localized UDP-D-xylose 4-epimerase encoded by the MUR4 gene of *Arabidopsis*. *Plant Cell* **15**, 523–531
2. Mølhøj, M., Verma, R., and Reiter, W.-D. (2004) The biosynthesis of D-galacturonate in plants. Functional cloning and characterization of a membrane-anchored UDP-D-glucuronate 4-epimerase from *Arabidopsis*. *Plant Physiol*. **135**, 1221–1230
3. Münster, A.K., Eckhardt, M., Potvin, B., Mühlenhoff, M., Stanley, P., and Gerardy-Schahn, R. (1998) Mammalian cytidine 5'-monophosphate N-acetylneuraminic acid synthetase: a nuclear protein with evolutionarily conserved structural motifs. *Proc. Natl. Acad. Sci. USA* **95**, 9140–9145
4. Capasso, J.M. and Hirschberg, C.B. (1984) Mechanisms of glycosylation and sulfation in the Golgi apparatus: evidence for nucleotide sugar/nucleoside monophosphate

and nucleotide sulfate/nucleoside monophosphate antiports in the Golgi apparatus membrane. *Proc. Natl. Acad. Sci. USA* **81**, 7051–7055
5. Ishida, N. and Kawakita, M. (2004) Molecular physiology and pathology of the nucleotide sugar transporter family (SLC35). *Pflugers Arch. Eur. J. Physiol.* **447**, 768–775
6. Ward, J.M. (2001) Identification of novel families of membrane proteins from the model plant *Arabidopsis thaliana*. *Bioinformatics* **17**, 560–563
7. Knappe, S., Flügge, U.I., and Fischer, K. (2003) Analysis of the plastidic phosphate translocator gene family in *Arabidopsis* and identification of new phosphate translocator-homologous transporters, classified by their putative substrate-binding site. *Plant Physiol.* **131**, 1178–1190
8. Bakker, H., Routier, F., Oelmann, S., Jordi, W., Lommen, A., Gerardy-Schahn, R., and Bosch, D. (2005) Molecular cloning of two *Arabidopsis* UDP-galactose transporters by complementation of a deficient Chinese hamster ovary cell line. *Glycobiology* **15**, 193–201
9. Baldwin, T.C., Handford, M.G., Yuseff, M.I., Orellana, A., and Dupree, P. (2001) Identification and characterization of GONST1, a golgi-localized GDP-mannose transporter in *Arabidopsis*. *Plant Cell* **13**, 2283–2295
10. Norambuena, L., Marchant, L., Berninsone, P., Hirschberg, C.B., Silva, H., and Orellana, A. (2002) Transport of UDP-galactose in Plants. *J. Biol. Chem.* **277**, 32923–32929
11. Norambuena, L., Nilo, R., Handford, M., Reyes, F., Marchant, L., Meisel, L., and Orellana, A. (2005) AtUTr2 is an *Arabidopsis thaliana* nucleotide sugar transporter located in the Golgi apparatus capable of transporting UDP-galactose. *Planta* **222**, 521–529
12. Rollwitz, I., Santaella, M., Hille, D., Flügge, U.I., and Fischer, K. (2006) Characterization of AtNST-KT1, a novel UDP-galactose transporter from *Arabidopsis thaliana*. *FEBS Lett.* **580**, 4246–4251
13. Bakker, H., Routier, F., Ashikov, A., Neumann, D., Bosch, D., and Gerardy-Schahn, R. (2008) A CMP-sialic acid transporter cloned from *Arabidopsis thaliana*. *Carbohydr. Res.* **343**, 2148–2152
14. Murashige, T. and Skoog, F. (1962) A revised medium for rapid growth and bio-assays with tobacco tissue culture. *Physiol. Plantarum.* **15**, 473–497
15. Takashima, S., Abe, T., Yoshida, S., Kawahigashi, H., Saito, T., Tsuji, S., and Tsujimoto, M. (2006) Analysis of sialyltransferase-like proteins from *Oryza sativa*. *J. Biochem.* **139**, 279–287
16. Segawa, H., Kawakita, M., and Ishida, N. (2002) Human and *Drosophila* UDP-galactose transporters transport UDP-N-acetylgalactosamine in addition to UDP-galactose. *Eur. J. Biochem.* **269**, 128–138
17. Ishida, N., Miura, N., Yoshioka, S., and Kawakita, M. (1996) Molecular cloning and characterization of a novel isoform of the human UDP-galactose transporter, and of related complementary DNAs belonging to the nucleotide-sugar transporter gene family. *J. Biochem.* **120**, 1074–1078
18. Deutscher, S.L. and Hirschberg, C.B. (1986) Mechanism of galactosylation in the Golgi apparatus. *J. Biol. Chem.* **261**, 96–100
19. Ito, H., Fukuda, Y., Murata, K., and Kimura, A. (1983) Transformation of intact yeast cells treated with alkali cations. *J. Bacteriol.* **153**, 163–168
20. Ishida, N., Kuba, T., Aoki, K., Miyatake, S., Kawakita, M., and Sanai, Y. (2005) Identification and characterization of human Golgi nucleotide sugar transporter SLC35D2, a novel member of the SLC35 nucleotide sugar transporter family. *Genomics* **85**, 106–116
21. Ishida, N., Ito, M., Yoshioka, S., Sun-Wada, G.-H., and Kawakita, M. (1998) Functional expression of human Golgi CMP-sialic acid transporter in the Golgi complex of a transporter-deficient Chinese hamster ovary cell mutant. *J. Biochem.* **124**, 171–178
22. Sun-Wada, G.-H., Yoshioka, S., Ishida, N., and Kawakita, M. (1998) Functional expression of the human UDP-galactose transporters in the yeast *Saccharomyces cerevisiae*. *J. Biochem.* **123**, 912–917
23. Takashima, S., Seino, J., Nakano, T., Fujiyama, K., Tsujimoto, M., Ishida, N., and Hashimoto, Y. (2009) Analysis of CMP-sialic acid transporter-like proteins in plants. *Phytochemistry* **70**, 1973–1981
24. Eckhardt, M., Gotza, B., and Gerardy-Schahn, R. (1999) Membrane topology of the mammalian CMP-sialic acid transporter. *J. Biol. Chem.* **274**, 8779–8787
25. Aoki, K., Ishida, N., and Kawakita, M. (2001) Substrate recognition by UDP-galactose and CMP-sialic acid transporters. *J. Biol. Chem.* **276**, 21555–21561
26. Aoki, K., Ishida, N., and Kawakita, M. (2003) Substrate recognition by nucleotide sugar transporters. *J. Biol. Chem.* **278**, 22887–22893
27. Bernsel, A., Viklund, H., Hennerdal, A., and Elofsson, A. (2009) TOPCONS: consensus prediction of membrane protein topology. *Nucleic Acids Res* **37**, (Web Server issue), W465–W468
28. Bernsel, A., Viklund, H., Falk, J., Lindahl, E., von Heijne, G., and Elofsson, A. (2008) Prediction of membrane-protein topology from first principles. *Proc. Natl Acad. Sci. USA* **105**, 7177–7181
29. Viklund, H. and Elofsson, A. (2004) Best α-helical transmembrane protein topology predictions are achieved using hidden Markov models and evolutionary information. *Protein Sci.* **13**, 1908–1917
30. Viklund, H. and Elofsson, A. (2008) A method that improves topology prediction for transmembrane proteins by using two-track ANN-based preference scores and an improved topological grammar. *Bioinformatics* **24**, 1662–1668
31. Granseth, E., Viklund, H., and Elofsson, A. (2006) ZPRED: Predicting the distance to the membrane center for residues in α-helical membrane proteins. *Bioinformatics* **22**, e191–e196
32. Hessa, T., Meindl-Beinker, N.M., Bernsel, A., Kim, J., Sato, Y., Lerch-Bader, M., Nilsson, I., White, S.H., and von Heijime, G. (2007) Molecular code for transmembrane–helix recognition by the Sec61 translocon. *Nature* **450**, 1026–1030
33. Berninsone, P., Eckardt, M., Gerardy-Schahn, R., and Hirschberg, C. (1997) Functional expression of the murine Golgi CMP-sialic acid transporter in *Saccharomyces cerevisiae*. *J. Biol. Chem.* **272**, 12616–12619
34. Reyes, F., Marchant, L., Norambuena, L., Nilo, R., Silva, H., and Orellana, A. (2006) AtUTr1, a UDP-glucose/UDP-galactose transporter from *Arabidopsis thaliana*, is located in the endoplasmic reticulum and up-regulated by the unfolded protein response. *J. Biol. Chem.* **281**, 9145–9151
35. Reyes, F., León, G., Donoso, M., Brandizzi, F., Weber, A.P., and Orellana, A. (2010) The nucleotide sugar transporters AtUTr1 and AtUTr3 are required for the incorporation of UDP-glucose into the endoplasmic reticulum, are essential for pollen development and are needed for embryo sac progress in *Arabidopsis thaliana*. *Plant J.* **61**, 423–435

36. Jackson, M.R., Nilsson, T., and Peterson, P.A. (1990) Identification of a consensus motif for retention of transmembrane proteins in the endoplasmic reticulum. *EMBO J.* **9**, 3153–3162
37. Kabuß, R., Ashikov, A., Olemann, S., Gerardy-Schahn, R., and Bakker, H. (2005) Endoplasmic reticulum retention of the large splice variant of the UDP-galactose transporter is caused by a dilysine motif. *Glycobiology* **15**, 905–911
38. Chenna, R., Sugawara, H., Koike, T., Lopez, R., Gibson, T.J., Higgins, D.G., and Thompson, J.D. (2003) Multiple sequence alignment with the Clustal series of programs. *Nucleic Acids Res.* **31**, 3497–3500
39. Page, R.D.M. (1996) TREEVIEW: an application to display phylogenetic trees on personal computers. *Comp. Appl. Biosci.* **12**, 357–358